# Neural Network Control for a Semi-Active Vehicle Suspension with a Magnetorheological Damper

D. L. GUO
*Key Laboratory of Smart Materials and Structures, Nanjing University of Aeronautics and Astronautics, Nanjing, China*
*Laboratory of Complex Systems and Intelligence Science, Institute of Automation, Chinese Academy of Sciences, Beijing, China*

H. Y. HU
*Key Laboratory of Smart Materials and Structures, Nanjing University of Aeronautics and Astronautics, Nanjing, China*

J. Q. YI
*Laboratory of Complex Systems and Intelligence Science, Institute of Automation, Chinese Academy of Sciences, Beijing, China*

(Received ; accepted )

*Abstract:* Semi-active vehicle suspension with magnetorheological dampers is a promising technology for improving the ride comfort of a ground vehicle. However, the magnetorheological damper always exhibits nonlinear hysteresis between its output force and relative velocity, and additional nonlinear stiffness owing to the state transition from liquid to semi-solid or solid, so that the semi-active suspension with magnetorheological dampers features nonlinearity by nature. To control such nonlinear dynamic systems subject to random road roughness, in this paper we present a neural network control, which includes an error back propagation algorithm with quadratic momentum of the multilayer forward neural networks. Both the low frequency of road-induced vibration of the vehicle body and the fast response of the magnetorheological damper enable the neural network control to work effectively on-line. The numerical simulations and an experiment for a quarter-car model indicate that the semi-active suspension with a magnetorheological damper and neural network control is superior to the passive suspensions in a range of low frequency.

*Key Words:* Semi-active control, neural networks, magnetorheological damper, vehicle suspension, vibration isolation



## 1. INTRODUCTION

Ground vehicles are always subject to the random excitation of an irregular road profile and undergo random vibrations. The random vibrations are harmful to ride comfort and the durability of the vehicle itself. To reduce random vibrations, great efforts have been made to develop various vehicle suspensions. However, a passive suspension without automatic

*Journal of Vibration and Control,* **9:** 0000–0000, 2004 DOI: 10.1177/107754603038968

control only reaches the optimal reduction of vibration for certain road profiles, and does not work well for a vehicle running at different speeds and for a wide variety of road profiles (Taghirad Hamid and Esmailzadeh, 1998). Hence, the techniques of both active suspensions and semi-active suspensions (Krtolica and Hrovat, 1992; Hać, 1992) have received much attention since the 1980s. The active suspension compensates the motion of vehicle body through the use of hydraulic actuators and controllers, and consumes a large amount of energy. In a semi-active suspension, nevertheless, the dynamic properties of a few components are adjusted on-line and much less energy is required. Many studies have indicated that a well-designed semi-active suspension could achieve similar dynamic performances of an active one, but save a great deal of cost and energy (Spencer et al., 2000). Thus, the semi-active suspension is a promising technique.

The dashpot with adjustable orifices, which has been widely used in passive vehicles, may be problematic in terms of reliability and maintenance owing to the mechanical factors in the systems, such as friction, saturation, and nonlinearity. To speed up the response of a semi-active suspension to the variation of an irregular road profile, magnetorheological (MR) dampers have been used to replace the dashpots with adjustable orifices. The MR damper is a special actuator, which utilizes the MR fluid to produce the controllable damping force. The essential characteristic of an MR fluid is its ability in the reversible change of states from a linear viscous fluid to a semi-solid with controllable yielding strength within a few milliseconds when it is subject to a controlled magnetic field (Winslow, 1949). Thus, an MR damper is able to alter its apparent viscosity in a few milliseconds with the variation of control voltage so that the output force follows the control strategy very well. Because of the primary advantage of MR fluids that the ancillary power can be directly supplied from common and low-voltage sources, MR fluids appear to be a promising alternative to electrorheological fluids for use in semi-active suspensions (Spencer et al., 2000).

An MR damper usually exhibits two types of nonlinearity. One is the hysteresis between the output force and relative velocity. The soft iron particles dispersed in an MR fluid are magnetized due to the alternated current, and the magnetism of the particles cannot vanish immediately when the current disappears. Hence, the MR damper exhibits a nonlinear hysteretic property between the output force and the relative velocity. The other is the additional nonlinear stiffness owing to the state transition from liquid to semi-solid or solid. This additional stiffness increases the equivalent fundamental frequency of a controlled suspension such that the dynamic performance of controlled suspension may be poorer than expected. As a result, the semi-active suspension with any MR damper is a nonlinear dynamic system by nature. It is not easy, and even impossible, to apply the traditional control strategies on the basis of precise mathematical models to the semi-active suspension equipped with MR dampers subject to random road roughness.

To attack the above problem, this study aims at the neural network control of a quarter-car model of semi-active suspension with an MR damper. The paper begins with the description of a quarter-car model with an MR damper and the random road roughness in Section 2. In Section 3, we present a neural network control strategy, that is, an indirect adaptive neural controller, which incorporates a neural identifier and an error estimator (Ghaboussi, 1995; Mistry et al., 1996). This control strategy can well estimate the back propagation error for the neural network controller in virtue of the neural network identifier. In Sections 4 and 5 we give the numerical simulations and experimental results of the new control strategy to verify the efficacy of the control strategy.

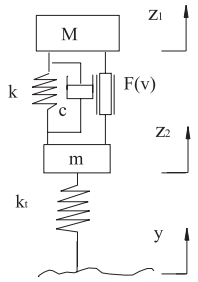


Figure 1. A quarter-car model of semi-active suspension.

## 2. THEORETICAL MODEL

### *2.1. Quarter-Car Model for Semi-Active Suspension*

The ride comfort of a vehicle mainly depends on the vertical vibration of the vehicle body. In studying the vertical vibration, the vehicle is usually simplified as a quarter-car model of two degrees of freedom, as shown in Figure 1, where an RD-1005 MR damper made in Lord is introduced to generate the control force so as to reduce the vibration of the vehicle body.

In this quarter-car model, $M$ and $m$ representing the mass of the vehicle body and the unsprung mass, such as the wheel and axle, can only move vertically under the excitation of road roughness $y$. The corresponding displacements are $z_1$ and $z_2$, respectively. The passive suspension, i.e. the uncontrolled suspension, consists of a linear spring of stiffness $k$ and a linear dashpot of damping $c$. In addition, $k_t$ is the stiffness of the tire, and the damping of the tire is negligible. Furthermore, $F(v)$ is the output force of the MR damper corresponding to input voltage $v$. The dynamic equation of this model reads

$$\begin{cases} M\ddot{z}_1 + c(\dot{z}_1 - \dot{z}_2) + k(z_1 - z_2) = F(v), \\ m\ddot{z}_2 - c(\dot{z}_1 - \dot{z}_2) - k(z_1 - z_2) + k_t z_2 = k_t y - F(v). \end{cases} \tag{1}$$

Figure 2 shows the configuration of the RD-1005 MR damper, where a piston with the throttle orifices and surrounding windings is the mobile part in the damper. When the piston moves up or down, the volume difference caused by the single-pole cylinder for the MR fluid may produce an instantaneous hydraulic impact. To avoid this impact, a nitrogen accumulator is installed at the bottom of the damper to compensate the volume difference. As experimentally identified in Weng et al. (2000), the output force $F(v)$ of the RD-1005 MR damper at input voltage $v$ yields

$$\begin{aligned} F(v) &= 247 + \frac{1.51}{1 + 10.34\mathrm{e}^{-1.04v}}\dot{z} \\ &+ \frac{2}{\pi}\frac{710}{1 + \mathrm{e}^{-1.1(v-2.3)}}\tan^{-1}\left[0.0725\left(\dot{z} - \frac{40\mathrm{sgn}\ddot{z}}{1 + 1.81\mathrm{e}^{-0.2v}}\right)\right], \end{aligned} \tag{2}$$

where $z = z_1 - z_2$ is the input relative displacement between the two ends of the damper.

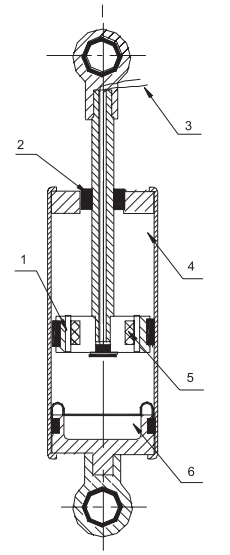


Figure 2. Configuration of a Lord RD1005 MR damper.

Given the road roughness $y$ in the time domain and the input voltage $v$ from the controller, it is easy to compute the dynamic response of the quarter-car model of semi-active suspension through the use of any available numerical solver, such as the Runge–Kutta algorithm, of ordinary differential equations.

### *2.2. Excitation Due to Road Roughness*

The simple road profiles, such as sinusoidal waves and saw-tooth waves, provide basic inputs to a ground vehicle for the evaluation of road disturbances in most studies on active or semi-active suspensions, but they do not offer any information about the effect of irregular road profiles on the actual dynamic behavior of a vehicle suspension. In this subsection, therefore, we present a brief description of irregular road profiles based on the International Organization for Standardization (ISO).

Figure 3 shows the classification of road roughness proposed by the ISO using the statistic power spectrum density (PSD). As most energy of a typical road spectrum falls into the range of low frequency, the PSD of road-test roughness denoted by $y$ is usually expressed as

$$S_{yy}\ (\Omega) = C_{SP}\ \Omega^{-2}, \tag{3}$$

where $C_{SP}$ represents the coefficient of road roughness, and $\Omega$ is the space frequency of road roughness, namely, the reciprocal of wavelength, which is usually in the interval of 0.01–2.83 $\mathrm{m}^{-1}$.

From the relation between the PSD $S_{yy}\ (\Omega)$ and the corresponding Fourier spectrum $Y(\Omega)$ of $y$ in the spatial frequency domain, the amplitude $|Y(\Omega)|$ of the Fourier spectrum

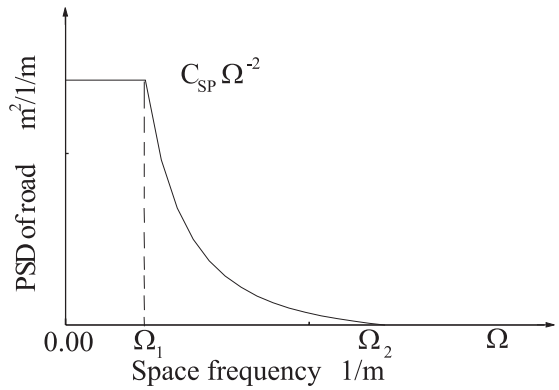


Figure 3. Spatial spectrum of road roughness.

of the road roughness can be determined. The random characteristic of a road profile requires that the phase $\arg[Y(\Omega)]$ of the Fourier spectrum of the road roughness must be stochastic since the corresponding amplitude $|Y(\Omega)|$ is deterministic. In this study, a uniformly distributed random phase $\arg[Y(\Omega)]$ is assumed in the interval $[-\pi, \pi]$. Therefore, the time history $y(t)$ of road disturbance can be computed by using the inverse Fourier transform as follows

$$y(t) = \sum_{f=l}^{h} Y(f)\, \mathrm{e}^{2\pi \Delta f t}\, \Delta f, \tag{4}$$

where $f$, the frequency of road roughness in time domain, is the product of the space frequency $\Omega$ and the speed $V$ of the vehicle. The lower and upper limits $l$ in $h$ the integral give the frequency range. In the following sections, the time series of road roughness $y(t)$ will be used as the road excitation applied to the tire of the vehicle model.

## 3. CONTROL STRATEGY

### *3.1. Neural Network Control*

The adaptive control focuses on the determination of the input signal of control in comparison with the reference signal. As is well known, it is extremely difficult to establish an accurate and simple mathematical model for a ground vehicle subject to the random road roughness. Thus, it is almost impossible to determine the input of control for reducing the random vibration of a semi-active suspension. One way of solving this tough problem is neural network control. Direct neural network control takes the error between the ideal reference signal and the system response as the error of back propagation. However, this error does not offer good information for updating the weights of neural networks. It is inaccurate and even uncontrollable to use the output errors as the errors of back propagation because of possible uncertainty of the nonlinear quarter-car model with semi-active suspension subject to the random road roughness.

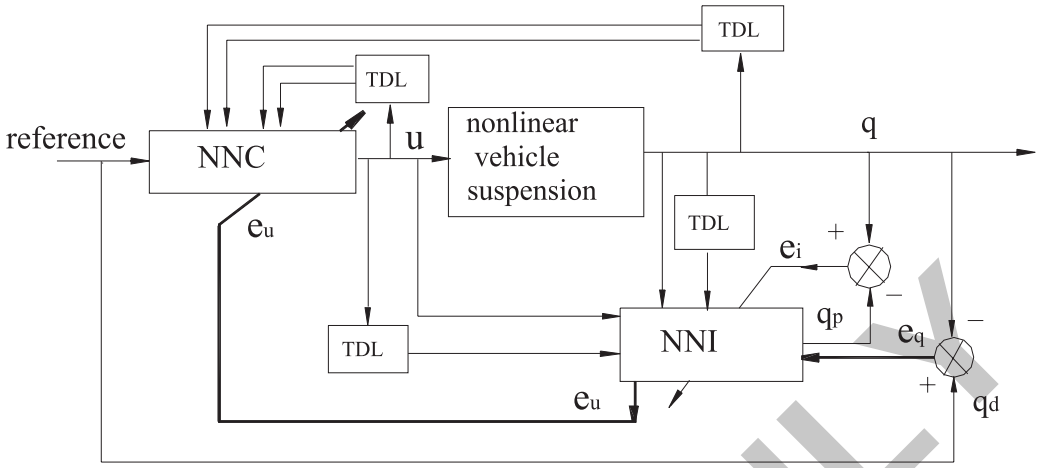


Figure 4. Structure of indirect adaptive control based on neural networks.

In this section we present an indirect adaptive control strategy based on the dynamic neural networks to well approximate the input error. Figure 4 shows the structure of the neural network control, where NNC is the abbreviation for neural network controller, NNI is the abbreviation for neural network identifier, and TDL is the abbreviation for tapped delay line. The NNC here has a single output since the input voltage of the MR damper is a unique control variable. As is well known, it is almost impossible to determine the ideal input $u_d$ of control because the inverse model of a nonlinear dynamic system is usually not available. Hence, the error $u_d - u$ for training the NNC cannot be achieved directly. In this study, the NNI not only traces the system response, but also computes the back propagation error for NNC units. Hence, the indirect adaptive strategy differs from the direct adaptive strategy.

The topological structure of the NNC consists of three layers with $4 \times 9 \times 1$ nodes, including one hidden layer only, while the NNI has the same structure as the NNC. The inputs to the networks are $\ddot{z}_1(k-1)$, $\ddot{z}_1(k)$, $u(k-1)$, $u(k)$, which are the system output and the control input at the previous sampling instant. The Sigmoid function serves as the activation function of the hidden and output layers. In Figure 4, the bold path indicates the direction of the training errors of the NNC.

In Figure 4, the output error $e_q$ between the reference signal $q_d$ and the system response $q$ reads $e_q \equiv q_d - q$. Hence, the control process diverges when the following performance index

$$J \equiv \frac{1}{2} e_q^2 = \frac{1}{2} (q_d - q)^2 \tag{5}$$

approaches the minimum. To minimize $J$, $e_q$ can be inversely propagated from the output layer to the input nodes of the NNI. Thus, the training control error $e_u$ becomes available. As a control error, $e_u$ is a better approximation than the direct difference between the reference and the response. Therefore, it is used to train and correct the NNC in control.

In the process of computing the control error $e_u$, the weights of NNI are updated on-line according to the error $e_i$ between the system response and the NNI output $q - q_p$ in order to

identify and trace the vehicle suspension. Because the NNI can be trained in advance, less correction is needed in the control process. This procedure, therefore, does not take much more time than the training process of using the error $q_d - q_p$ directly. For comparison, the strategy, which takes $q_d - q_p$ directly as the training error, is called a direct NNC for short.

For a neural network control, the control error $e_u$ in an indirect NNC is more accurate than the direct error and is a better approximation to the truer value. While the NNI is trained successfully, the errors propagated back to its input layer are indeed the training errors of the NNC.

### *3.2. Selecting and Updating Weights*

To start the control, the initial weights are randomly selected from the interval [0, 1]. The algorithm of updating weights is the following BP algorithm with quadratic momentum terms

$$\Delta\omega(k) = -\eta\frac{\partial J}{\partial\omega} + \alpha\Delta\omega(k-1) + \beta\Delta\omega(k-2) \tag{6}$$

where $\eta$ is the learning rate, and $\alpha$ and $\beta$ are the momentum factors. All these parameters are assumed to be positive. The function of quadratic momentum terms here is as follows. For the controller without any momentum terms, the weights to be updated increase with an increase of parameter $\eta$. Thus, excessively large $\eta$ will make the activation function saturated. Otherwise, the convergence may become very slow if $\eta$ is too small. The quadratic momentum terms can enlarge the learning rate, but hardly lead to oscillation. In particular, the quadratic momentum term $\beta$ can serve as a simulated process of annealing to speed up the convergence rate for neural networks. Thus, the proportional value of a previously updated weight is added to the weight to be updated. That is, this weight updating procedure includes the information of previous updating of weights. In addition, the entire computations for error back propagation and weight updating are similar to the general BP algorithm.

In addition, the successive control process and the very large assemblage of input samples require selecting pattern manners. That is, the weights are updated and the weight errors are computed while each pattern is dealt with. Before handling the next pattern, the varied weights are added to the previous weights.

## 4. NUMERICAL SIMULATIONS

In order to verify the efficacy of the new control strategy, a number of numerical simulations were made for the quarter-car model equipped with an MR damper. To obtain an agreement with further experiment, the fundamental natural frequency of the quarter-car model was chosen as 1.8 Hz. In the simulations, the Runge–Kutta algorithm written in Turbo-C code was used to compute the dynamic response of vehicle subject to the road disturbance of C grade. The random excitation of an irregular road profile is given by equation (4) on the basis of the road classification of the ISO database.

Figure 5 shows the vertical accelerations of the vehicle body in the time domain for the quarter-car model without control and with indirect NNC, as well as the control voltage input to the MR damper in semi-active suspension. Compared with Figure 5(a), the vertical acceleration in Figure 5(c) was considerably reduced. The root-mean-square (rms) accelerations of the vehicle body in these two cases were 4.11 and 2.02 m $s^{-2}$, respectively.

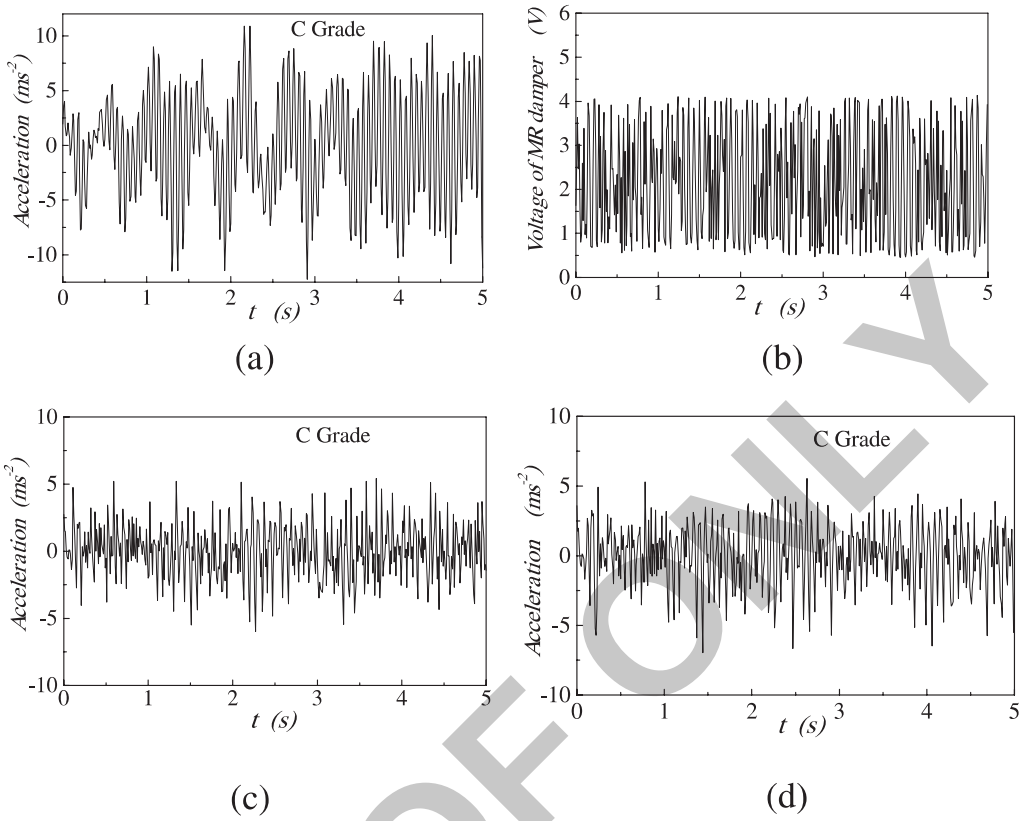


Figure 5. Comparison of time histories of uncontrolled and controlled responses of a vehicle body in a numerical simulation: (a) without control; (b) control voltage of an MR damper; (c) under indirect NNC; (d) under indirect NNC without quadratic momentum.

Figure 5(d) shows the time history of vertical acceleration under indirect NNC without quadratic momentum and the corresponding rms acceleration is 2.98 m $s^{-2}$. This result obviously validated the conclusion that the quadratic momentum is able to optimize the control error and increase the control effect. Therefore, the new control strategy is superior to the traditional ones.

## 5. AN EXPERIMENTAL STUDY

### *5.1. Experimental Setup*

Although the neural network control has proved its applicability to many industrial processes, the computational time of control strategy for acceptable convergence often becomes a bottleneck in the application of active control of vibration. However, the low frequency of road excitation and the quick response of MR dampers make a real-time NNC possible for the semi-active suspension with an MR damper.

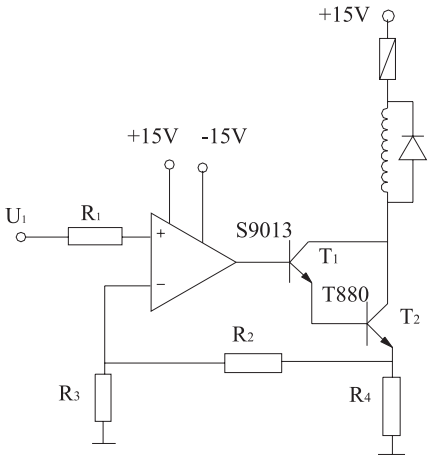


Figure 6. Circuit of current amplifier for an MR damper.

In the experiment, the computer works in a multi-task circumstance with the help of a counter/timer 8253. The entire process of control begins with a sampling step. When the sampling step terminates, the counter/timer 8253 calls an interruption of the CPU so that the CPU reads the sampled data. As soon as the reading step is over, the CPU turns to the computation of control strategy. During the computation, the next sampling step is being on. For the vibration control of vehicle suspension, the interval of sampling is long enough to compute the convergent weighs of neural networks. For example, when the sampling frequency is selected as 200 Hz, i.e. 10 times as high as the maximal excitation frequency, an interval of 5 ms is available for the computation of the NNC. Once the neural networks converge in computation of control strategy, the control signal is output simultaneously to the MR damper. Consequently, the acceleration of the vehicle body tends to be reduced at this control step. The acceleration of the vehicle body is reduced step by step with the above procedure being repeated.

An important issue in the experimental setup is the design of a practical current amplifier for the MR damper. Figure 6 shows the circuit of current amplifier for the RD-1005 MR damper, where the cement resistance $R_4$ acts as the output pole to boost the capability of loading. This current amplifier worked well for the fast intensity change of magnetic field for the MR damper in the experiment, but is still subject to further improvement so as to be powered by batteries of 12 V on vehicles.

### *5.2. Experimental Results*

To verify the applicability of the control strategy and real-time realization, an experiment was made on a test rig of the quarter-car model. The fundamental natural frequency of the model is 1.8 Hz, and the corresponding stiffness of passive suspension is 17500 N m$^{-1}$. As a comparison, the direct NNC was also applied to the model. In the direct NNC, the control errors $\bar{e}_u$ are defined as the difference between the desired $q_d$ and the output of the identified model $q_p$, i.e. $\bar{e}_u \equiv q_d - q_p$, which is not similar to the indirect control error $e_u$.

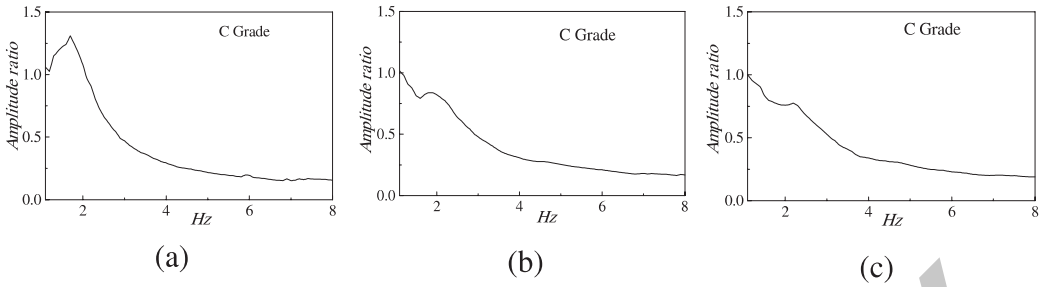


Figure 7. Comparison of Fourier spectra of uncontrolled and controlled responses of a vehicle body: (a) without control; (b) under direct NNC; (c) under indirect NNC.

Figure 7 shows the Fourier spectra of the acceleration of the vehicle body without control, with direct NNC and indirect NNC, respectively. Figures 7(b) and (c) indicate that the semi-active suspension under indirect NNC with quadratic momentum is superior to the direct strategy in the entire frequency range we are concerned with. The isolation performance is particularly pronounced at the resonant frequency of the vehicle body. Compared with the numerical simulations, the isolation performance in the experiment was not so good. The main cause might come from the extra harmonic components of excitation produced by the hydraulic shaker.

When the winding current of the MR damper increases, the MR fluid changes its state from liquid into semi-solid or solid. Meanwhile, the additional stiffness accompanying the hysteretic damping force occurs so that the stiffness of an MR damper under control becomes much larger than the traditional vibration damper, where the additional stiffness is negligible. Thus, the vehicle body can be rigidly joined together with the unsprung mass when the winding current of MR damper is excessively large. As a result, the kinetic status of the vehicle body and the tire will tend gradually to be in-phase. In this case, the additional stiffness increases the stiffness of whole suspension, and the fundamental frequency of suspension system as well.

Figure 8 shows the Fourier spectrum of vertical acceleration for the vehicle body excited at a resonant frequency of 1.8 Hz. Figure 8 shows that the harmonic component of tripled fundamental frequency was considerably strengthened under control. Especially, the harmonic components of fundamental frequency and the corresponding multiple frequencies in Figure 8(b) were all enlarged due to the additional nonlinear stiffness of the MR damper. Therefore, the additional nonlinear stiffness of the MR damper decreases the control effect and worsens the effect of vibration isolation.

## 6. CONCLUSIONS

In this paper we present a semi-active suspension on the basis of neural network control and MR damper for the vibration control of a quarter-car model of vehicle suspension. The new control strategy works very fast since the neural networks include a single hidden layer only and the neural network identifier receives good training prior to the control. The numerical simulations and an experiment show that the semi-active suspension with new control strategy

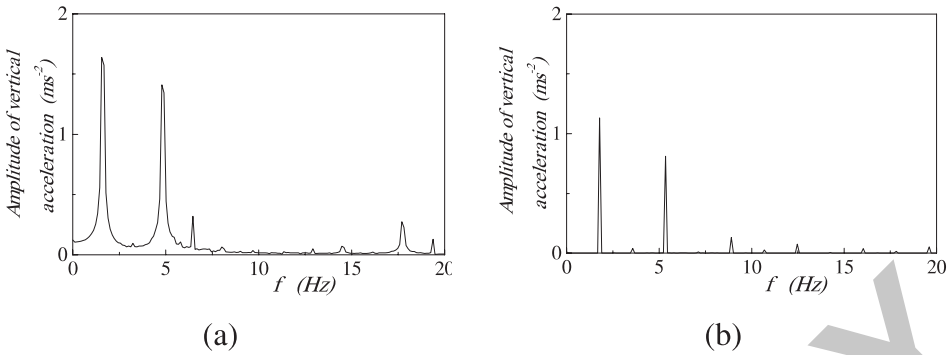


Figure 8. Effect of additional nonlinear stiffness of an MR damper: (a) without control; (b) under control.

is superior to the passive suspensions and the semi-active suspensions with current neural network control. Compared with a passive suspension, for example, the rms acceleration of the vehicle body subject to the random road disturbance of C grade was reduced by 38.2% when the direct neural network control was used, and by 55% when the indirect adaptive neural network control was implemented in numerical simulations. In comparison with the passive suspension, the semi-active suspension with indirect adaptive control of neural networks reduced the acceleration of the vehicle body under the sinusoidal road excitation of C grade by 41% in an experiment.

*Acknowledgments. This research was supported in part by the National Natural Science Foundation of China under Grants Nos 50135030 and 59625511.*

## REFERENCES

Ghaboussi, J., 1995, "Active control of structures using neural networks," *Journal of Engineering Mechanics* **121**(4), 555–567.

Hać, A., 1985, "Suspension optimization of a 2-DOF vehicle model using a stochastic optimal control technique," *Journal of Sound and Vibration* **100**(3), 343–357.

Hać, A., 1992, "Optimal linear preview control of active vehicle suspension," *Vehicle System Dynamics* **21**, 167–195.

Krtolica, R. and Hrovat, D., 1992, "Optimal active suspension based on a half-car model: an analytical solution," *IEEE Transactions on Automatic Control* **137**(4), 528–532.

Mistry, S. I., Chang, S. L., and Nair, S. S., 1996 "Indirect control of a class of nonlinear dynamic systems," *IEEE Transactions on Neural Networks* **7**(4), 1015–1023.

Spencer, B. F. Jr, Johnson, E. A., and Ramallo, J. C., 2000, "Smart isolation for seismic control," *JSME International Journal (Series C)* **43**(3), 704–711.

Taghirad Hamid, D. and Esmailzadeh, E., 1998, "Automobile passenger comfort assured through LQG/LQR active suspension," *Journal of Vibration and Control* **4**, 603–618.

Weng, J. S., Hu, H. Y., and Zhang, M. K., 2000, "Experimental modeling of magnetorheological damper," *Journal of Vibration Engineering* **13**(4), 616–620.

Winslow, W. M., 1949, "Contributed original research," *Journal of Applied Physics* **20**, 1137–1140.

Yu, Z. S., 1981, *Theory of Automobiles*, Mechanical Industry Press, Beijing.